Available online at www.sciencedirect.com
SCIENCE DIRECT®
Toxicology Letters 155 (2005) 377–384
Toxicology Letters
www.elsevier.com/locate/toxlet

Multi-walled carbon nanotube interactions with human epidermal keratinocytes☆

Nancy A. Monteiro-Riviere[a,*], Robert J. Nemanich[b], Alfred O. Inman[a], Yunyu Y. Wang[b], Jim E. Riviere[a]

[a] *Center for Chemical Toxicology Research and Pharmacokinetics, North Carolina State University, 4700 Hillsborough Street, Raleigh, NC 27606, USA*
[b] *Department of Physics, North Carolina State University, Raleigh, NC 27606, USA*

Received 12 October 2004; received in revised form 12 November 2004; accepted 12 November 2004

Abstract

Carbon nanotubes have widespread applications in multiple engineering disciplines. However, little is known about the toxicity or interaction of these particles with cells. Carbon nanotube films were grown using a microwave plasma enhanced chemical vapor deposition system. Human epidermal keratinocytes (HEK) were exposed to 0.1, 0.2, and 0.4 mg/ml of multi-walled carbon nanotubes (MWCNT) for 1, 2, 4, 8, 12, 24 and 48 h. HEK were examined by transmission electron microscopy for the presence of MWCNT. Here we report that chemically unmodified MWCNT were present within cytoplasmic vacuoles of the HEK at all time points. The MWCNT also induced the release of the proinflammatory cytokine interleukin 8 from HEKs in a time dependent manner. These data clearly show that MWCNT, not derivatized nor optimized for biological applications, are capable of both localizing within and initiating an irritation response in a target epithelial cell that composes a primary route of occupational exposure for manufactured nanotubes.

Keywords: Multi-wall carbon nanotubes; Human epidermal keratinocytes; Transmission electron microscopy; IL-8

1. Introduction

There has been explosive growth in engineering disciplines using nanoparticles, structures with characteristic dimensions between 1 and 100 nm. These range from applications in the fields of ceramics to microelectronics as well as many areas of drug delivery (Jortner and Rao, 2002; Zhan et al., 2003; Bogunia-Kubik and Sugisaka, 2002). The unique phys-

☆ Portions of this work were presented at the Second Annual National Academies Keck Futures Initiative Conference Designing Nanostructures at the Interface between Biomedical and Physical Systems, Irvine, CA, 18–21 November 2004.

* Corresponding author. Tel.: +1 919 513 6426; fax: +1 919 513 6358.
E-mail address: nancy_monteiro@ncsu.edu (N.A. Monteiro-Riviere).
URL: http://cctrp.ncsu.edu (N.A. Monteiro-Riviere).

0378-4274/$ – see front matter © 2004 Elsevier Ireland Ltd. All rights reserved.
doi:10.1016/j.toxlet.2004.11.004

ical properties of nanoparticles (conductivity, reactivity) compared to larger microparticles enable these novel engineering applications. One of the principal attributes of nanoparticles enabling development is their unique catalytic properties. Modifications, including end-of-tube or sidewall derivatization, modify their physical properties and alter solubility or dispersion.

Nanoparticles, when engineered appropriately, exhibit a variety of unique and tunable chemical and physical properties. These characteristics have made engineered nanoparticles central components in an array of emerging technologies. These unique properties may also result in similarly unique biological effects. Although they have widespread potential applications in material sciences and engineering, the toxicology of these components has not been thoroughly evaluated under environmental and occupational exposure scenarios. A major issue is the health impact to humans exposed to nanomaterials by oral, dermal or inhalational routes.

There is limited literature available on the toxicology of unmodified manufactured nanoparticles (Baron et al., 2002; Dagani, 2003). The pulmonary toxicity of carbon nanotubes has been reported after intratracheal instillation to mice and rats (Warheit et al., 2004; Lam et al., 2004). The primary finding of these studies was the formation of epithelial granulomas and inflammation depending on the type of particle used. An important observation was if carbon nanotubes reach the lung tissue, they were more toxic than either carbon black or quartz dust, two known pulmonary toxicants (Nikula et al., 1995; Driscoll et al., 1996). This may be secondary to the tendency of these particles to self-aggregate when removed from controlled conditions.

There have been reports of dermal irritation in humans after exposure to carbon fibers (carbon fiber dermatitis, hyperkeratosis) (Eedy, 1996). A recent study suggests that nanoparticles may be toxic to immortalized HaCaT human keratinocyte cultures (Shvedova et al., 2003). These data suggest that nanotubes, not optimized for cellular delivery, altered keratinocyte function. Since there is limited information on how nanotubes can react with living cells, the objective of this study was to assess the interaction between multi-walled carbon nanotubes (MWCNT) and human epidermal keratinocytes (HEK) using transmission electron microscopy (TEM) and the release of the proinflammatory cytokine interleukin (IL) 8 as an early marker of biological response. Cell culture studies were conducted to assess the potential hazard of MWCNT exposure to cells. The actual risk after in vivo topical exposure would be dependent upon absorption, which was not assessed in this study.

2. Materials and methods

The vertically aligned carbon nanotube films were grown using a microwave plasma enhanced chemical vapor deposition system. The alignment of the MWCNT in this system is attributed to the electric field at the edge of the plasma (Bower et al., 2000). The same growth chamber is also used to grow diamond films (Köck et al., 2004). The catalyst was an 80 nm iron film deposited on 2.5 cm silicon wafers by DC magnetron sputtering. The iron-coated silicon substrates were introduced in the reactor that was pumped to a base pressure of less than 1×10^{-3} Torr, with the working pressure maintained at 20 Torr. The growth temperature (900 °C) was achieved through heating from induction and microwave plasma. The ammonia and acetylene precursors were introduced into the chamber at a flow rate of 70 and 18 sccm, respectively, and the plasma ignited (600 W) for 30 min.

Two- and three-dimensional atomic force microscope images of the iron film surface were obtained with the Thermo Microscope M5 model in contact mode (Fig. 1a). The sputtered iron surface (no pretreatment) had island-like structures approximately 100 nm in diameter with a surface height of approximately 3 nm. These structures act as carbon nanotube nucleation centers in the growth phase. The nanotube films were characterized using scanning electron microscopy (SEM) and high-resolution transmission electron microscopy (HRTEM). An SEM image of the aligned nanotube film was obtained with a JEOL 6400 (Fig. 1b). The film was grown perpendicular to the substrate with an approximate thickness of 50 μm and an approximate average diameter of 100 nm. The yield was relatively high, with a density of 1×10^{10} nanotubes/cm^2. The HRTEM images depict multi-walled structures that resemble a ‘bamboo’ shoot (Fig. 1c). The intergraphitic layers between two compartments have up to 30 sheets, with a thickness of about 12 nm (Fig. 1d). These multi-

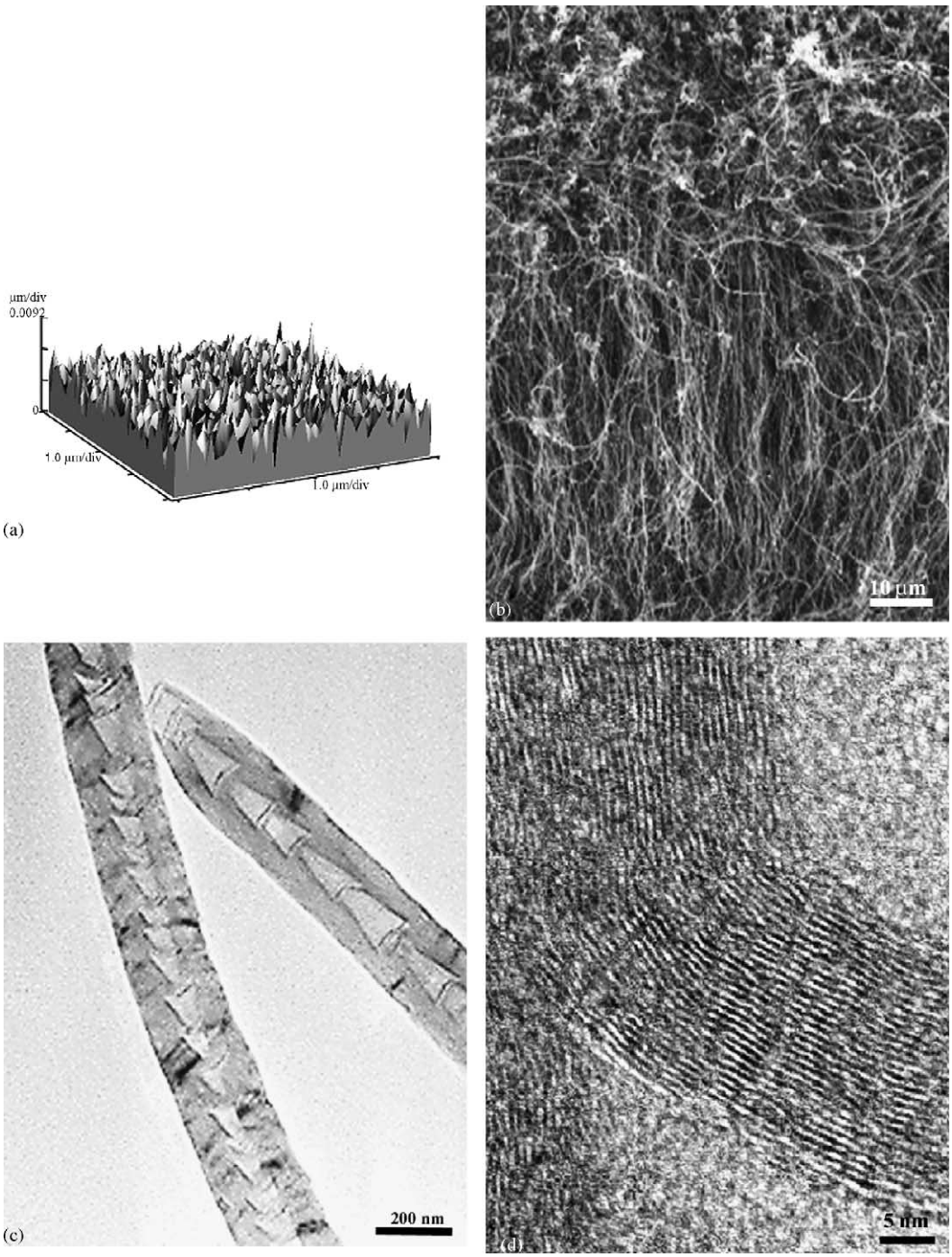

Fig. 1. Characterization of multi-walled carbon nanotubes. (a) Atomic force image of the iron film surface. (b) SEM image of the aligned carbon nanotube film. Note the film was grown perpendicular to the substrate. (c) HRTEM depicting the multi-walled structures resembling bamboo shoots. (d) TEM depicting the intergraphic layers between the two compartments showing many sheets and thickness.

walled nanotubes have an internal structure that approaches that of carbon fibers. Auger electron spectroscopy found no detectable iron at the film surface. The technique is sensitive to a depth of approximately 2 nm from the exposed surface, and has a sensitivity of less than 1%. The results support a prior study that indicated base growth mode for these MWCNT (Wang et al., 2004). The MWCNT were removed from the growth surface by manual scraping with a metal blade.

On average, 5 mg of MWCNT were scraped from each silicon wafer. To visualize nanotubes within keratinocytes using TEM, cryopreserved pooled human neonatal epidermal keratinocytes (HEK) (BioWhittaker, Inc., Walkersville MD) were seeded in cell culture flasks (25 cm^2; ~100,000 cells) and grown to 80% confluency at 37 °C in a humidified 5% CO_2 environment. MWCNT (0.4 mg/ml) were thoroughly suspended by sonication for 5 min in keratinocyte growth medium (KGM-2). Sonification was used previously to prepare MWCNT for TEM characterization, and there was no evidence that the process led to breaking or defect formation in the MWCNT (Wang et al., 2004). The HEKs were treated for 1, 4, 8, 12, 24 and 48 h, harvested by trypsinization (0.25%) and/or scraping, rinsed in Hank's balanced salt solution (HBSS), and fixed in Trump's fixative at 4 °C. Cells were then rinsed in 0.1 M phosphate buffer (pH 7.2), pelleted in a microcentrifuge tube, and embedded in 3% molten agar. In order to maintain a monolayer to confirm the intracellular localization of MWCNT, additional cells were grown on 60 mm Permanox dishes (Electron Microscopy Sciences, Fort Washington, PA), and treated for 24 h with 0.4 mg/ml nanotubes; one plate of HEKs were treated as above, and the other plate was treated with the nanotube solution filtered through a 0.2 μm filter to eliminate aggregated particles. With treatment termination, the medium from all cells was harvested and stored at −80 °C until assayed. The HEKs were rinsed in HBSS and fixed in Trump's fixative at 4 °C. The cells in agar as well as the cell monolayers (attached to Permanox plates) were post-fixed in 1% osmium tetroxide (Polysciences, Inc., Warrington, PA) in 0.1 M sodium phosphate buffer, dehydrated through graded ethanol solutions, cleared in acetone, and infiltrated and embedded in Spurr's resin. Thin sections (800–1000 Å) were mounted on copper grids and examined on a Philips EM208S transmission electron microscope operating at an accelerating voltage of 80 kV. Stained (lead citrate and uranyl acetate) and unstained cells were examined for the presence of the MWCNT.

To determine the distribution of MWCNT across cells, approximately 50 cells treated with the 0.4 mg/ml dose for 24 and 48 h were counted randomly. To further verify that iron was not present within the MWCNT located within the cytoplasmic vacuoles, elemental analysis was conducted using a JEOL 6400F Field Emission scanning electron microscope equipped with an EDS detector operating at an accelerating voltage of 3 kV. The sensitivity of this method of analysis is 1%. Cells exposed to MWCNT were analyzed on carbon-coated grids with a formvar-coated film.

In order to assess a biological effect of MWCNT on keratinocytes, cells were plated in 96-well culture plates (0.32 cm^2 growth area) at a density of approximately 7000 cells per well. Upon reaching 80% HEK confluency, each 96-well plate was exposed to MWCNT in KGM-2, as well as media alone, which served as the controls. Immediately prior to treating the cells, nanotubes were added to the KGM-2 to provide a 0.4 mg/ml stock solution. The solution was thoroughly sonicated to disperse the structures. From this stock, serial dilutions of 0.2 and 0.1 mg/ml nanotubes were prepared and used to treat the cells. The HEK medium was harvested at 1, 2, 4, 8, 12, 24 and 48 h post-treatment (four wells/plate/time point), and stored at −80 °C until assayed. HEKs in the 24 h or 48 h wells were assayed for viability using neutral red (NR) as described previously (Borenfreund and Puerner, 1984, 1985; Chou et al., 2002). Since the residual nanotubes can affect the absorbance values, the solution in each well was pipetted into a new 96-well plate. Absorbance, directly proportional to cell viability, was determined spectrophotometrically at 550 nm in an ELISA plate reader (Multiskan RC, Labsystems, Helsinki, Finland). The media was assayed in triplicate for IL-8 using a human IL-8 cytoset (Biosource International, Camarillo, CA). The mean IL-8 concentration (pg/ml) for each treatment and time point was calculated (Chou et al., 2002). The IL-8 concentration and cell viability of the treatments were statistically compared using ANOVA (SAS 6.12 for Windows; SAS Institute, Cary, NC). Multiple comparisons among different treatments were conducted within each exposure length and sampling time using the Student's *t*-test at the $P < 0.05$ level of significance.

3. Results

These data clearly show chemically unmodified nanotube localization within HEKs. The morphology of keratinocytes exposed to MWCNT was different from that of the control. The nuclei of the cells were free of MWCNT, but numerous vacuoles were present within the cytoplasm. Many of the cytoplasmic vacuoles contained MWCNT of various sizes, up to 3.6 μm in length. In addition, MWCNT were found within the free cytoplasm and, at times, were seen lying close to the nucleus and appeared to pierce the nuclear membrane. Nanotubes were primarily located within the intracytoplasmic vacuoles of the keratinocytes (Fig. 2a). This intracellular location was confirmed in the cell monolayer cultures (Fig. 2b), a technique which assures that particles are within the cells and are not an artifact due to plane of section. This intercellular localization is again clearly evident in Fig. 3a. Higher magnification of the intracytoplasmic vacuole (Fig. 3b) shows that nanotubes within cells preserved the typical multi-walled 'bamboo' shoot structure seen after synthesis (Fig. 1c).

The nanotubes were more numerous within cells as treatment concentration and exposure time increased. The number of keratinocytes containing MWCNT increased from 59.1% at 24 h to 84.0% at 48 h at the 0.4 mg/ml dose. It is interesting to note that when filtered media was used for dosing, the larger MWCNT aggregates were removed to prevent these aggregates and long MWCNT from being available to the HEKs. In this dosing scenario, MWCNT up to 0.2 μm

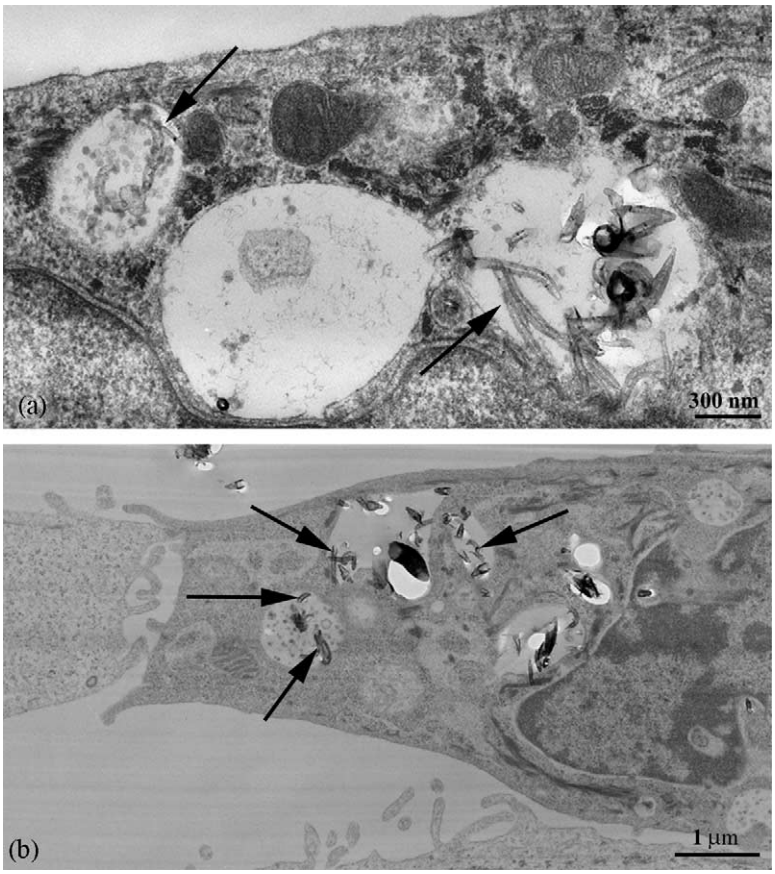

Fig. 2. Transmission electron micrograph of human epidermal keratinocytes. (a) Intracellular localization of the MWCNT. Arrows depict the MWCNT present within the cytoplasmic vacuoles of a HEK. (b) Keratinocyte monolayer grown on a Permanox surface. Arrows depict the intracytoplasmic localization of the MWCNT.

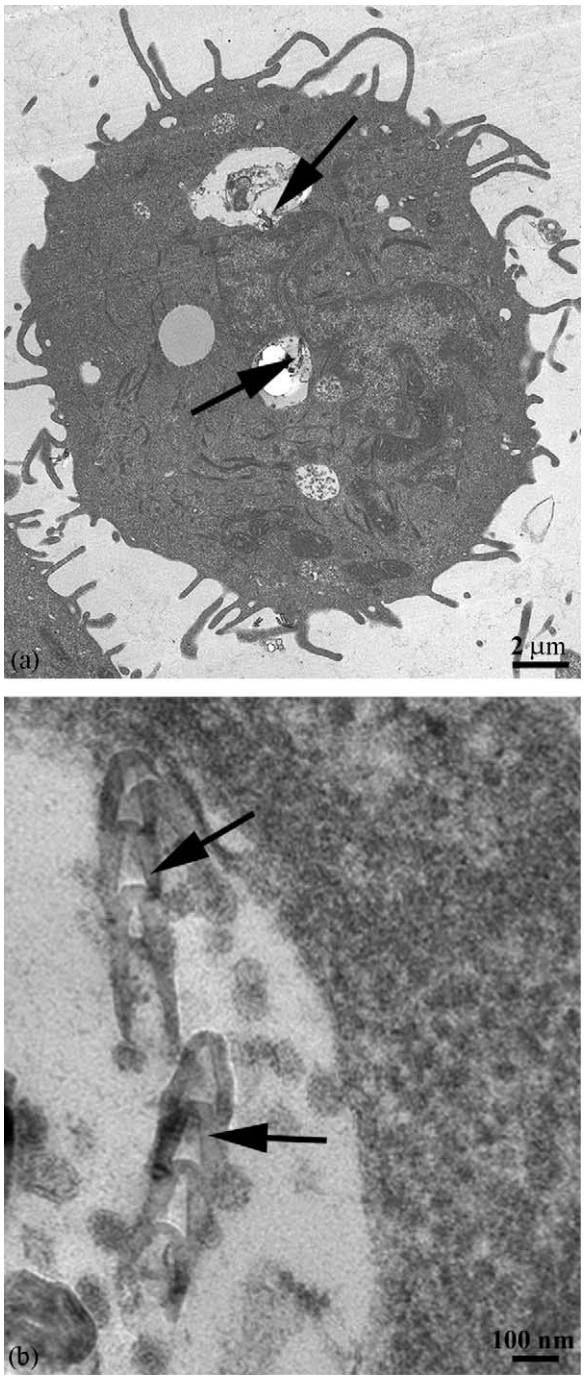

Fig. 3. Transmission electron micrograph of human epidermal keratinocytes. (a) Low magnification of a keratinocyte for precise location of the vacuoles containing MWCNT (arrows). (b) High magnification of vacuole to demonstrate that MWCNT retain their structure.

in length were still present in only a few isolated cells.

Elemental analysis was performed on discrete nanotubes at 100,000× in the cells exposed to 0.4 mg/ml of MWCNT to exclude the possibility of the iron catalyst as a contaminant of the MWCNT. The presence of electron-dense MWCNT against the low contrast cell background made it easy to conduct the elemental analysis of the MWCNT within unstained cells. Only carbon, not iron, was present above background signal.

HEK viability assessed by the NR assay slightly decreased in a dose-dependent manner at 24 h (Fig. 4a) and 48 h (data not shown) after exposure to the nanotubes. The concentration of IL-8 increased with time (Fig. 4b). By 8 h, IL-8 concentration in the media from the treated HEKs was significantly greater ($P < 0.05$) than in the controls. A clear dose response was seen through 24 h. IL-8 release is typically higher in the cells treated with 0.4 mg/ml MWCNT compared to the lower concentrations. Consistent with this pattern, the HEKs treated with filtered nanotube medium contained fewer nanotubes, and the IL-8 concentration was comparable to the controls (data not shown).

4. Discussion

A great deal of attention has been focused on determining the properties of nanoparticles that might serve as efficient drug delivery matrices (Bogunia-Kubik and Sugisaka, 2002; Jores et al., 2003). Chemically functionalized, water-soluble single-walled carbon nanotubes have been shown to enter fibroblasts (Pantarotto et al., 2004), promyelocytic leukemia (HL60) cells and T cells (Kam et al., 2004). However, little to no attention has been paid to the ability of unmodified nanotubes, manufactured for engineering applications, to localize within cells. Evidence of dermal irritation (Eedy, 1996) coupled with a report of toxicity to keratinocytes (Shvedova et al., 2003) suggests that particles not optimized for intracellular delivery may enter cells and adversely affect cellular function. We used a relatively complex MWCNT in these studies as a model of a structure not designed for biological applications. TEM confirmed that MWCNT without chemical modification nor adjuvant treatments (vehicles, surfactants, other solubilization strategies) are capable of entering HEK. An increase in the release of IL-8 from treated

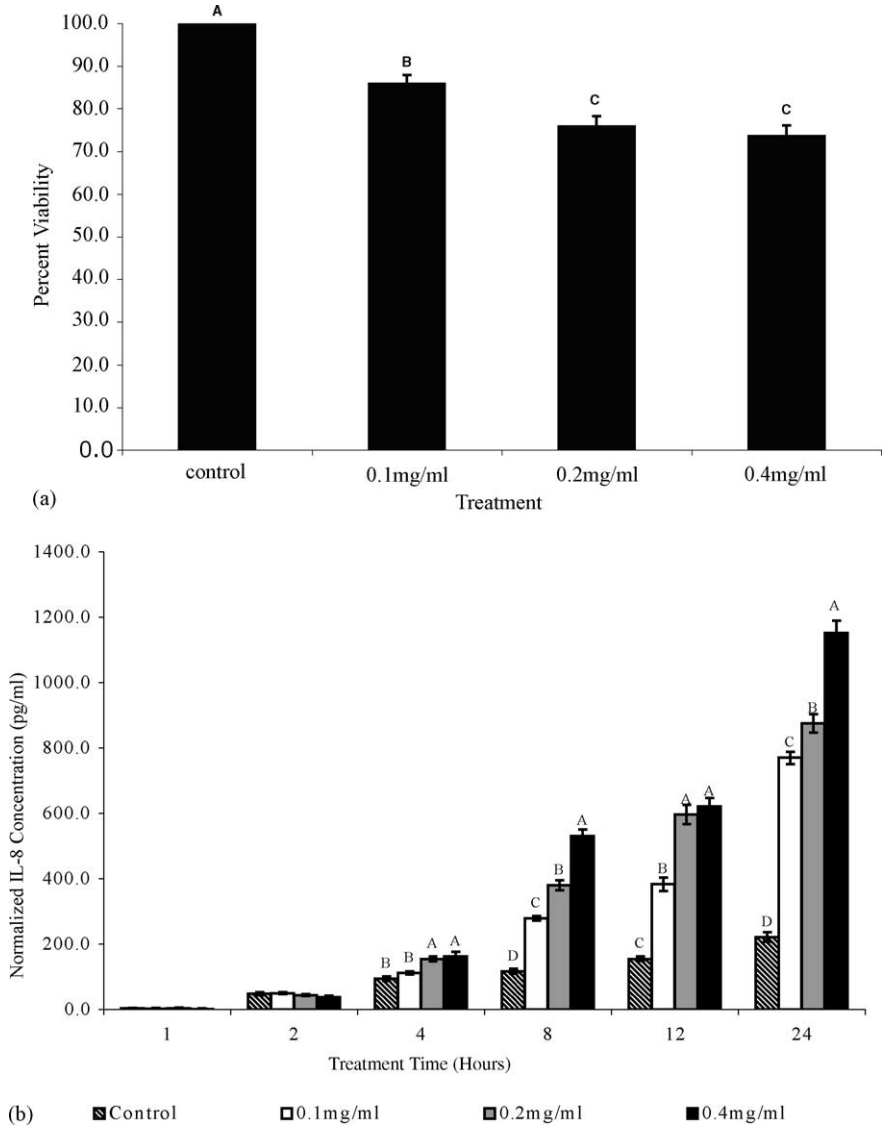

Fig. 4. Graphs illustrating the effect of multi-walled carbon nanotubes on keratinocyte viability and IL-8 release. (a) Mean viability (±S.E.M.) of the HEKs 24 h following exposure to MWCNT. Note the decrease in viability with an increase in MWCNT concentration. Histogram with different letters (A, B, and C) denote mean values that are statistically different at $P < 0.05$. (b) Mean ± S.E.M. IL-8 increases with time and concentration of MWCNT. Histogram with different letters (A–D) denote mean values that are statistically different at $P < 0.05$.

cells confirmed that a biological response had occurred (Chou et al., 2002). However, this response may be the cumulative effect of both MWCNT attaching to the plasma membrane as well as being internalized by the cell. This marker of irritation (IL-8) is consistent with reports of dermal irritation in humans. Finally, this response is not due to the presence of the iron catalyst, since iron was not detected in the MWCNT before or after exposure using two independent techniques.

These studies were not designed to develop a precise dose–response relationship for nanotube exposure, nor define the relation of nanotube properties (surface properties, size, etc.) to cellular penetration. It was obvious in our exposures that the vast majority of nan-

otubes dosed in the media did not interact with keratinocytes. However, up to 84% of 0.4 mg/ml treated keratinocytes were involved by 48 h. Although only relatively short nanotubes (up to 3.6 μm in length) were observed within cells, this could be due to plane of section which does not allow for three dimensional visualization of longer, more tortuous MWCNT. As is typically seen with these structures, clumping and aggregation occurred during exposure. However, after filtering out large aggregates, nanotubes were still present within the keratinocytes.

MWCNTs are capable of entering human keratinocytes as well as eliciting a biological effect manifested by IL-8 release. The mechanism of both penetration and effect remains to be elucidated. Our data does not provide information as to whether such structures are a risk to occupationally exposed persons since keratinocyte cultures lack the protective stratum corneum barrier seen with intact skin. The importance of these findings is that a detectable fraction of chemically unmodified MWCNT are capable of intracellular localization as well as causing irritation in keratinocytes. In short, keratinocytes can be affected by MWCNT. Exposure must be evaluated before the risk of this hazard can be determined in an occupational or environmental scenario. These findings suggest that the toxicology of these structures must be assessed before widespread public exposure so that appropriate protective measures can be developed.

References

Baron, P.A., Maynard, A., Foley, M., 2002. Evaluation of aerosol release during the handling of unrefined single walled carbon nanotube material. NIOSH Dart-02-191, National Institute of Occupational Safety and Health, Cincinnati, OH, NTIS PB 2003-102401.

Bogunia-Kubik, K., Sugisaka, M., 2002. From molecular biology to nanotechnology and nanomedicine. BioSystems 65, 123–138.

Borenfreund, E., Puerner, J., 1984. A simple quantitative procedure using monolayer cultures for cytotoxicity assays (HTD/NR-90). J. Tiss. Cult. Meth. 9, 7–9.

Borenfreund, E., Puerner, J., 1985. Toxicity determined in vitro by morphological alterations and neutral red absorption. Toxicol. Lett. 24, 119–124.

Bower, C., Zhu, W., Jin, S., Zhou, O., 2000. Plasma-induced alignment of carbon nanotubes. Appl. Phys. Lett. 77, 830–832.

Chou, C.C., Riviere, J.E., Monteiro-Riviere, N.A., 2002. Differential relationship between the carbon chain length of jet fuel aliphatic hydrocarbons and their ability to induce cytotoxicity vs. interleukin-8 release in human epidermal keratinocytes. Toxicol. Sci. 69, 226–233.

Dagani, R., 2003. Nanomaterials: safe or unsafe? CENEAR 81, 30–33.

Driscoll, K.E., Carter, J.M., Howard, B.W., Hassenbein, D.G., Pepelko, W., Baggs, R.B., Oberdorster, G., 1996. Pulmonary inflammatory, chemokines, and mutagenic responses in rats after subchronic inhalation of carbon black. Toxicol. Appl. Pharmacol. 136, 372–380.

Eedy, D.J., 1996. Carbon-fibre-induced airborne irritant contact dermatitis. Contact Dermatitis 35, 362–363.

Jores, K., Mehnert, W., Mäder, K., 2003. Physiochemical investigations on solid lipid nanoparticles and on oil-loaded solid lipid nanoparticles: a nuclear magnetic resonance and electron spin resonance study. Pharm. Res. 20, 1274–1283.

Jortner, J., Rao, C.N.R., 2002. Nanostructured advanced materials. Perspectives and directions. Pure Appl. Chem. 74, 1491–1506.

Kam, N.W.S., Jessop, T.C., Wender, P.A., Dai, H., 2004. Nanotube molecular transporters: internalization of carbon nanotube-protein conjugates into mammalian cells. J. Am. Chem. Soc. 126, 6850–6851.

Köck, F.A.M., Garguilo, J.M., Nemanich, R.J., 2004. Imaging electron emission from diamond film surfaces: N-doped diamond vs. nanostructured diamond. Diamond Relat. Mater. 10, 1714–1718.

Lam, C.W., James, J.T., McCluskey, R., Hunter, R.L., 2004. Pulmonary toxicity of single-wall carbon nanotubes in mice 7 and 90 days after intratrachael instillation. Toxicol. Sci. 77, 126–134.

Nikula, K.J., Snipes, M.B., Barr, E.B., Griffifth, W.C., Henderson, R.F., Mauderly, J.L., 1995. Comparative pulmonary toxicities and carcinogenicities of chronically inhaled diesel exhaust and carbon black in F344 rats. Fundam. Appl. Toxicol. 25, 80–94.

Pantarotto, D., Briand, J.P., Prato, M., Bianco, A., 2004. Translocation of bioactive peptides across cell membranes by carbon nanotubes. Chem. Commun. 1, 16–17.

Shvedova, A.A., Kisin, E.R., Murray, A.R., Gandelsman, V.Z., Maynard, A., Baron, P., 2003. Exposure to carbon nanotube material: assessment of nanotube cytotoxicity using human keratinocyte cells. J. Toxicol. Environ. Health A 66, 1909–1926.

Wang, Y.Y., Tang, G.Y., Koeck, F.A.M., Brown, B., Garguilo, J.M., Nemanich, R.J., 2004. Experimental studies of the formation process and morphologies of carbon nanotubes with bamboo mode structures. Diamond Relat. Mater. 13, 1287–1291.

Warheit, B.D., Laurence, B.R., Reed, K.L., Roach, D.H., Reynolds, G.A.M., Webb, T.R., 2004. Comparative pulmonary toxicity assessment of single-wall carbon nanotubes in rats. Toxicol. Sci. 77, 117–125.

Zhan, G.-D., Kuntz, J.D., Wan, J., Mukherjee, A.K., 2003. Single-wall carbon nanotubes a attractive toughening agents in alumina-based nanocomposites. Nat. Mater. 2, 38–42.